Topology of the C-Terminal Fragment of Human Presenilin 1

Young S. Oh* and R. James Turner

Membrane Biology Section, Gene Therapy and Therapeutics Branch, National Institute of Dental and Craniofacial Research, National Institutes of Health, DHHS, Bethesda, Maryland 20892

Received May 23, 2005; Revised Manuscript Received July 14, 2005

ABSTRACT: Mutations of human presenilin 1 (PS1) have been genetically linked to early-onset familial Alzheimer's disease. PS1 contains 10 hydrophobic regions (HRs) sufficiently long to be α-helical membrane spanning segments. Most previous topology studies agree that the N-terminus of PS1 is cytosolic and HRs 1−6 span the membrane but HR 7 does not. However, whether HRs 8 and 9 are membrane spanning segments remains controversial. Here we study the topology and biogenesis of this region of PS1 using a reporter gene fusion approach, where portions of the PS1 sequence containing possible membrane spanning segments were fused up- or downstream of a reporter sequence whose translocation into the endoplasmic reticulum could be monitored via its glycosylation. We provide strong evidence, supported by cysteine accessibility studies in full-length PS1, that HRs 8 and 9 are indeed membrane spanning and that the integration of HR 8 into the membrane is dependent on the presence of HR 9. We also explain how our results reconcile previous apparently divergent conclusions regarding the topology of HRs 8 and 9.

Mutations in the integral membrane protein presenilin 1 (PS1)[1] are the most common cause of early-onset familial Alzheimer's disease (*1*−*3*). In cells, PS1 assembles with three other integral membrane proteins, nicastrin, PEN-2, and APH-1, to form the γ-secretase complex (*3*). γ-Secretase is an aspartyl protease whose substrates are a number of type I transmembrane proteins (*4*) including the cell-fate-specifying receptor Notch and the Alzheimer's disease-associated β-amyloid precursor protein (APP). γ-Secretase is a member of a recently discovered novel class of proteases that cleave their substrates within the membrane (*4*). Mutations in PS1 associated with inherited Alzheimer's disease apparently lead to aberrant cleavage of APP, resulting in increased production of the longer neurotoxic form of β-amyloid found in the characteristic senile plaques observed in the brains of Alzheimer's patients (*1*, *2*, *5*).

PS1 is thought to be the catalytic subunit of the γ-secretase complex (*1*−*4*), and so the determination of its transmembrane topology is especially important to our understanding of its role in substrate binding, γ-secretase activity, and ultimately Alzheimer's disease. However, despite a number of studies, the topology of PS1 has remained controversial (reviewed in ref *6*). Hydropathy analysis shows that PS1 contains 10 hydrophobic regions (HRs) that could potentially form α-helical membrane spanning segments (MSSs; Figure 1A). From the results of experiments examining antibody epitope accessibility (*7*−*10*) and the membrane integration of truncated forms of PS1 (*11*, *12*) or SEL-12 (*13*, *14*), a PS1 homologue from *Caenorhabditis elegans*, there is a general consensus that HRs 1−6 are MSSs and that HR 7 is left out of the membrane so that the N-terminus of PS1 and the "loop" region between HRs 6 and 8 are on the same side of the membrane. All of these groups but one (*9*, *10*) have found that the N-terminus and loop are cytosolic. We recently reexamined this question by studying the accessibility of the N-terminus and loop region of endogenously expressed PS1 to proteinase K (*15*). We found that both of these regions were digested by proteinase K in intact cytosolic-side-out endoplasmic reticulum (ER) vesicles. Since the majority of the cellular PS1 is found in the ER (*16*−*18*), this result argues strongly that most PS1 molecules are indeed oriented with their N-termini and loop regions in the cytosol. In this same paper we applied three independent methodologies to investigate the location of HR 10 and the extreme C-terminus of PS1. In contrast to the conclusions of most previous studies, the results from all three of these methods indicated that HR 10 spans the membrane and that the C-terminal ∼14 amino acids of PS1 lie in the extracytoplasmic space.

In the present paper we examine the transmembrane topology of HRs 8 and 9 of human PS1, concerning which there is also disagreement. More specifically, in a paper published in 1997, Lehmann et al. (*11*) constructed a series of chimeric molecules in which a reporter peptide was fused to the PS1 sequence truncated after each HR. These constructs were then expressed in the presence of canine pancreatic microsomes or in COS cells, and the location of the reporter peptide inside or outside of the endoplasmic reticulum (ER) lumen was assayed on the basis of its glycosylation and sensitivity to protease digestion. These authors concluded that HRs 8 and 9 were not MSSs and that both were located in the cytosol along with HR 7. Using a similar approach in 1999, Nakai et al. (*12*) also concluded that HRs 8 and 9 were cytosolic, but they also found that HR 9 could not be extracted from the membrane by an

* Address correspondence to this author at Building 10, Room 1A01, 10 Center Drive, MSC 1190, National Institutes of Health, Bethesda, MD 20892-1190. Tel: (301) 594-1652. Fax: (301) 402-1228. E-mail: yoh@mail.nih.gov.

[1] Abbreviations: PS1, presenilin 1; HR, hydrophobic region; APP, β-amyloid precursor protein; ER, endoplasmic reticulum; MSS, membrane spanning segment; PNGase F, peptide:*N*-glycosidase F.

10.1021/bi0509494
Published on Web 08/13/2005

alkaline wash and proposed that, although it was not a MSS, it was tightly bound to the membrane on the cytosolic side. Li and Greenwald (*13*, *14*) studied the topology of the PS1 homologue SEL-12 by fusing β-galactosidase to the SEL-12 sequence truncated after each of the HRs. These constructs were then expressed in vivo in *C. elegans*. Since β-galactosidase is only active within the cytoplasm of cells, its location and thereby the topology of SEL-12 could be deduced from its activity. In contrast to the results of Lehmann et al. (*11*) and Nakai et al. (*12*) these authors concluded that HRs 8 and 9 of SEL-12 were MSSs (*13*). They also carried out similar experiments expressing human PS1/β-galactosidase fusion proteins in *C. elegans* and likewise concluded that HRs 8 and 9 of PS1 were MSSs (*14*).

Here we provide additional strong evidence from mammalian cells that both HRs 8 and 9 of PS1 are MSSs and that their integration into the membrane involves the recently described phenomenon of "forced transmembrane orientation" (*19*, *20*). In addition, we indicate how our results reconcile the above apparently divergent conclusions regarding the topology of HRs 8 and 9.

MATERIALS AND METHODS

Clones. Human PS1 and AE1 clones were generously provided by Drs. Todd E. Golde (Mayo Clinic Jacksonville) and Reinhart Reithmeier (University of Toronto), respectively.

DNA Constructs. Segments of the human PS1 sequence were cloned into the mammalian expression vector pEGFP-β, whose construction has been described previously (*21*). This vector drives the expression of a fusion protein consisting of the enhanced green fluorescent protein (EGFP) followed by *Bgl*II and *Hin*dIII restriction sites for the insertion of additional sequence and a C-terminal glycosylation tag. The segments of PS1 indicated in the text and/or figure legends were amplified by PCR and cloned in frame into pEGFP-β by standard methods. The PCR primers, incorporating 5′ and 3′ *Bgl*II and *Hin*dIII sites, respectively, were designed essentially as reported in previous studies from our laboratory (*21*).

The mammalian expression vector PS1-HR9 coding for HR 9 of PS1 preceded by a glycosylation tag and followed by EGFP was constructed from three PCR products. The first consisted of amino acids D626−W662 of the human anion exchanger AE1 preceded by a *Bam*HI site and a start codon and followed by a *Bgl*II site. The second consisted of amino acids S397−P433 of human PS1 preceded by a *Bgl*II site and followed by a *Hin*dIII site. The third consisted of EGFP preceded by a *Hin*dIII site and followed by an *Xho*I site. These three PCR products were cloned in series between the *Bam*HI and *Xho*I sites of the expression vector pBK-CMV^{lac-} (Stratagene) prepared as described previously (*22*). The above AE1 sequence (D626−W662) represents the extracellular loop between MSSs 7 and 8 of this protein and contains a glycosylation site known to be utilized in AE1 (*23*). The plasmids PS1-HR1, PS1-HR2, and AE1-HR1 were constructed from PS1-HR9 by replacing the sequence of HR 9 with that of HR 1 of PS1 (E64−S105), HR 2 of PS1 (D110−A164), and HR 1 of AE1 (A400−G436), respectively (each generated by PCR).

Site-directed mutagenesis of PS1 was carried out using the Quikchange II XL kit (Stratagene) according to the manufacturer's instructions.

The correctness of all PCR products and mutants was confirmed by direct sequencing.

Growth and Transfection of HEK-293T and HEK-293 Cells. HEK-293T cells (from American Type Culture Collection) and HEK-293 cells (from Microbix Biosystems Inc.) were cultured and transfected as previously described (*24*). To obtain stably transfected HEK-293 cells, hygromycin B (0.1 mg/mL) was added to the medium 2 days after transfection, and cells were subcultured as necessary. Confluent cultures of hygromycin-resistant cells were obtained 2−3 weeks later.

Preparation of Particulate and Membrane Fractions. "Particulate fractions" from transiently transfected HEK-293T cells were obtained essentially as previously described (*21*). Briefly, cells were washed in PBS and then homogenized in ice-cold TEEA buffer consisting of 20 mM Tris-HCl, pH 8.0, 1 mM EDTA, 3 mM EGTA, 300 μM AEBSF (ICN), 10 μM leupeptin, 10 μM pepstatin A, and 2.5 μg/mL aprotinin (all from Boehringer-Mannheim). This homogenate was centrifuged at 1000*g* for 10 min and the supernate saved. The pellet was resuspended in TEEA buffer, rehomogenized, and centrifuged as before. The combined supernates from these two homogenization steps were centrifuged at 100000*g* for 30 min, and the resulting particulate fraction was resuspended in TEEA buffer, snap frozen, and stored at −70 °C. The protein concentration of these particulate fractions was typically 5−10 mg/mL, measured using the Bio-Rad protein assay kit.

The "membrane fraction" was prepared from the above particulate fraction by an alkaline flotation step (*15*, *19*, *21*, *25*) as follows. A 30−50 μg aliquot of the particulate fraction was diluted to 50 μL in 100 mM Na_2CO_3 (pH 11.5, final concentration). This mixture was incubated on ice for 30 min and then mixed with 90 μL of 2.5 M sucrose in 100 mM Na_2CO_3 (final sucrose concentration 1.6 M). Next, 70 μL of 1.25 M sucrose and 70 μL of 0.25 M sucrose, both in 100 mM Na_2CO_3 (pH 11.5), were overlaid on the 1.6 M sucrose mixture, and the tube was centrifuged at 100000*g* for 60 min in a Beckman TL100 ultracentrifuge equipped with a TLA100.3 rotor. The 0.25 and 1.25 M sucrose layers and the interface between the 1.25 and 1.6 M sucrose layers were recovered as the membrane fraction.

Deglycosylation of the Membrane Fraction. Deglycosylation of the membrane fraction by treatment with peptide: *N*-glycosidase F (PNGase F; New England Biolabs) was carried out as previously described (*21*).

Cysteine Derivatization. The procedure for cysteine derivatization was based on that of Feramisco et al. (*26*) with some modifications. Sealed cytosolic-side-out ER vesicles were prepared from HEK-293 cells stably transfected with wild-type or mutant PS1 (S367C or W404C) as previously described (*15*). Aliquots of this preparation (50−100 μg of protein, measured using the Pierce Micro BCA protein assay kit) suspended in buffer B (10 mM HEPES−KOH, pH 7.4, 10 mM KCl, 1.5 mM $MgCl_2$, 5 mM Na-EDTA, 5 mM Na-EGTA, 250 mM sucrose, and 100 mM NaCl plus Roche protease inhibitor cocktail no. 1836153) were incubated with 1−5 mM 2-(trimethylammonium)ethyl methanethiosulfonate (MTSET; Toronto Research Chemicals) for 10 min at room

temperature. These vesicles were then spun down at 20000*g* for 15 min, resuspended in 200 μL of buffer B, spun down again, resuspended in 100 μL of buffer B containing 1 mM biotin maleimide (Molecular Probes), and incubated for 30 min at 50 °C. After the biotinylation reaction was quenched with 20 mM β-mercaptoethanol for 2 min, the vesicles were collected by centrifugation, and the pellet was solubilized in 200 μL of buffer C (50 mM Tris-HCl, pH 7.4, 150 mM NaCl, 0.1% SDS, 1.5% NP-40, and Roche protease inhibitors). One hundred microliters of a 50% slurry of immobilized Neutravidin biotin binding protein (bound to agarose beads; Pierce) in buffer C was added to each sample and incubated for 1 h at room temperature with gentle shaking. After removal of the supernatant, the pelleted beads were washed four times in buffer C, resuspended in 40 μL of SDS loading buffer, and heated for 5 min at 100 °C. The eluted fraction of biotinylated proteins was subjected to SDS/PAGE and Western blot analysis.

SDS−PAGE, Western Blotting, and Data Analysis. SDS−PAGE and Western blotting were carried out as previously described (*15*, *21*) using a rabbit polyclonal antibody raised against GFP (Molecular Probes) or a mouse monoclonal antibody recognizing the C-terminal fragment of PS1 (Chemicon). Quantitation of Western blots was done using ImageQuant 5.2 software (Molecular Dynamics). The quantitative results shown are means ± SE for three or more independent experiments.

RESULTS AND DISCUSSION

MSS Predictions for PS1. Figure 1A shows a hydropathy plot for PS1 indicating its 10 HRs. As already discussed, there is general *experimental* agreement that the first 6 HRs span the membrane and that HR 7 does not. Most laboratories, including our own, agree that the N-terminus of PS1 is cytosolic and thus that HR 7 is also in the cytosol. Consistent with this, our previous experiments show that antibody epitopes located at the N-terminus of PS1 and in the loop between HRs 7 and 8 are digested by proteinase K in intact cytosolic-side-out ER vesicles (*15*). As we have previously noted (*15*), we cannot exclude the possibility that there is a pool of PS1 on the cell surface with an opposite orientation as proposed by Dewji and Singer (*9*, *10*); however, our results (*15*) indicate that the vast majority of PS1 molecules in the cell have their N-terminus and loop regions in the cytoplasm. In Figure 1B we illustrate the results of a number of recent theoretical methods for predicting transmembrane topology, all of which have been shown to be significantly more dependable than classical Kyte−Doolittle hydropathy analysis (see Figure 1 caption for references). All of these methods predict that HR 9 is membrane-spanning, consistent with its high hydrophobicity (Figure 1A); however, there is some disagreement regarding the disposition of HRs 7 and 8. Interestingly, all methods but one predict that HR 10 is membrane-spanning, consistent with our recent results (*15*). The amino acid sequence of the C-terminal region of PS1 indicating the *approximate* positions of HRs 7−10 is illustrated in Figure 1C.

Initial Results Concerning the Association of HRs 7−9 with the Membrane. In our initial experiments designed to explore the topology of HRs 7−9 of PS1 we used a truncation mutant approach where portions of the PS1

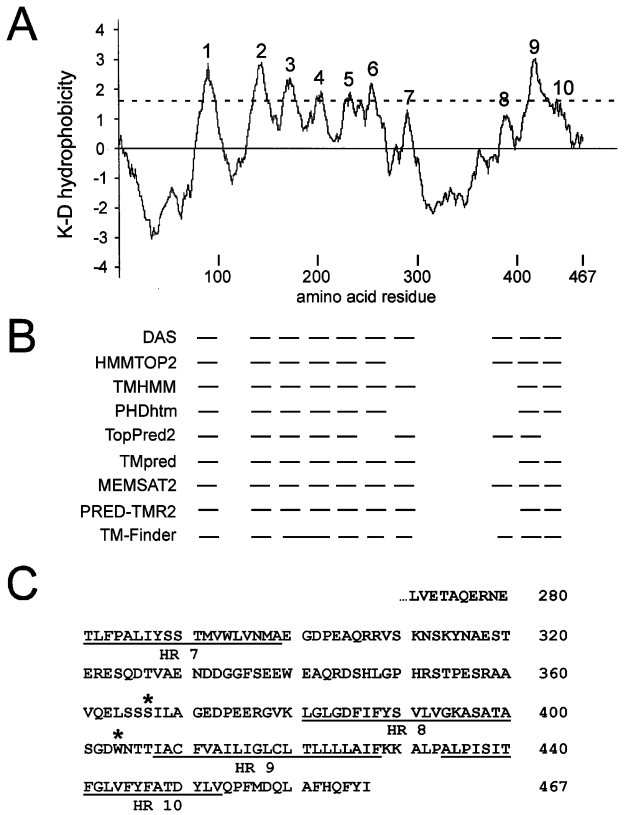

FIGURE 1: Hydrophobicity and MSS predictions for human PS1. (A) Hydrophobicity plot of human PS1 obtained using the method of Kyte and Doolittle (K-D) with a 19 amino acid window. The 10 hydrophobic regions (HRs) referred to in the text are indicated. The dashed line at an average hydrophobicity/residue of 1.6 is the value suggested by Kyte and Doolittle as the lower limit for a MSS (*35*). (B) Predicted MSSs from various theoretical methods available over the Internet. The references for the methods are as follows: DAS (*36*), HMMTOP2 (*37*), TMHMM (*38*), PHDhtm (*39*), TopPred2 (*40*), TMpred (*41*), MEMSAT2 (*42*), PRED-TMR2 (*43*), and TM-Finder (*44*). (C) C-Terminal sequence of PS1. The underlined amino acids indicate the approximate positions of HRs 7−10. Two residues mutated to cysteine for cysteine accessibility studies (Figure 6) are indicated by asterisks.

sequence containing possible MSSs were fused between EGFP and the extracellular tail (177 amino acids) of the β-subunit of the rabbit gastric H,K-ATPase, a glycosylation tag (see Materials and Methods). This latter sequence contains five consensus sites for N-linked glycosylation (*27*); when translocated into the interior of the ER, it acquires ~14 kDa of apparent molecular mass due to glycosylation, an increase that is easily discerned on SDS−PAGE (*21*, *24*, *28*). The use of this glycosylation tag in membrane topology determinations is now well established (*21*, *24*, *27*−*30*). EGFP provides a convenient marker for fusion protein detection on Western blots. In addition, this N-terminal EGFP moiety is expected to act as a "cytosolic anchor" that constrains the N-terminal end of the fusion protein to remain in the cytosol. This is because the synthesis and folding of EGFP into a stable compact structure precede the appearance of the HRs of the fusion protein from the ribosome; stably folded N-terminal moieties such as this have previously been shown to act as cytosolic anchors presumably because they are unable to pass though the translocon channel into the lumen of the ER (*31*, *32*).

In Figure 2A we illustrate the results of a series of experiments where PS1 fragments encoding HR 7 (cHR 7),

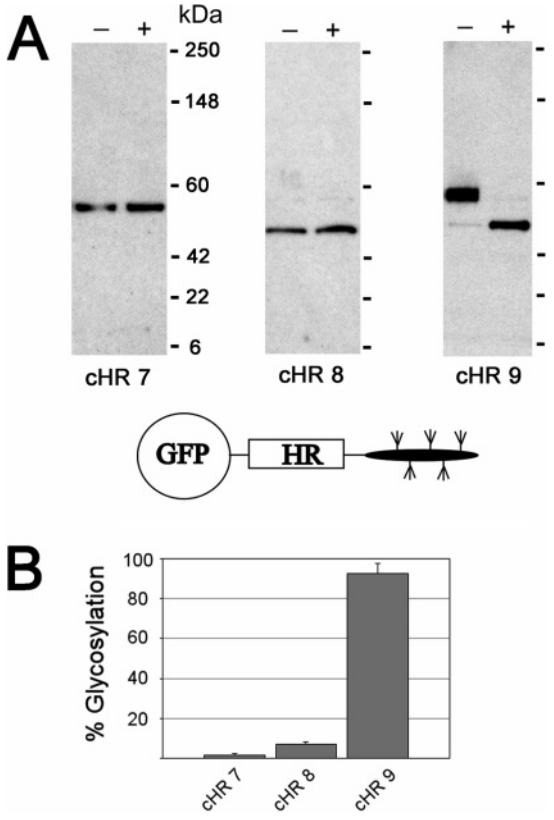

FIGURE 2: Membrane integration of PS1 HRs 7−9. (A) Typical Western blots of membrane fractions prepared from HEK-293T cells transfected with the constructs indicated. Membranes were treated with (+) or without (−) PNGase F. All procedures are described in Materials and Methods. A schematic representation of the fusion proteins is shown below the blots. (B) For each construct the density of the glycosylated band has been expressed as a percentage of the total recombinant protein ($n \geq 3$). The PS1 sequences cloned into pEGFP-β were L271−L369 (cHR 7), L364−D403 (cHR 8), and A398−P433 (cHR 9).

HR 8 (cHR 8), or HR 9 (cHR 9) were expressed as EGFP-β-subunit fusion proteins in HEK-293T cells. In each of the panels in Figure 2A we show the results of a typical experiment where the membrane fraction from HEK-293T cells, transiently transfected with the construct indicated, was treated with (+) or without (−) PNGase F (see Materials and Methods). These membrane fractions were run on SDS−PAGE and probed by Western blotting using an antibody against EGFP to determine the extent of glycosylation of the β-subunit and thus its location inside or outside the ER lumen. The percentage of glycosylated recombinant protein for each construct is shown in Figure 2B. Thus, for example, the fusion protein incorporating HR 9 is highly glycosylated (92.5 ± 4.8%), indicating that its C-terminus is exposed to the ER lumen. On the other hand, the proteins encoded by cHR 7 and cHR 8 show relatively little glycosylation, indicating that their C-termini are mainly in the cytosol. These data demonstrate that HR 9 is capable of integrating into the ER membrane in an N_{cyt}/C_{lum} orientation but that HRs 7 and 8 apparently cannot integrate into the membrane on their own, consistent with their rather low hydrophobicities (Figure 1A).

We next explored the biogenesis of PS1 downstream of HR 6 by adding successive HRs to the construct cHR 7 (Figure 3A) and examining the ability of the resulting fusion proteins to associate with the membrane. In membrane fractions from HEK-293T cells expressing these constructs we found that cHR 7−8 (containing HRs 7 and 8) was 7.2 ± 1.7% glycosylated, cHR 7−9 (containing HRs 7, 8, and 9) was 16% glycosylated, and cHR 7−10 (containing HRs 7, 8, 9, and 10) was 94% glycosylated (the latter two data are from Figure 3 of ref *15*). When the complete N-terminus of PS1 encoding HRs 1−6 was added to cHR 7−8 (cHR 1−8), cHR 7−9 (cHR 1−9), and cHR 7−10 (cHR 1−10), similar glycosylation patterns were obtained (data not shown and Figure 3 of ref *15*).

The glycosylation of cHR 7−10 and other data presented in ref *15* indicate that this recombinant protein is integrated into the membrane. On the other hand, the weak glycosylation of cHR 7−8 taken together with the results of Figure 2 and the low hydrophobicity of this region (Figure 1A) suggests that this construct is not membrane-integrated. Superficially, the weak glycosylation of cHR 7−9 might also be interpreted as indicating that HR 9 does not efficiently integrate into the membrane when it is expressed "in context" with its upstream sequence in PS1. However, because of the high hydrophobicity of HR 9 and its ability to integrate into the membrane on its own, documented in Figure 2, we felt that additional experiments were required to clarify its association with the membrane.

Recovery of Fusion Proteins in the Membrane Fraction. As detailed in Materials and Methods, the membrane preparations analyzed above were obtained from particulate fractions of HEK-293T cells using an alkaline flotation procedure. In this procedure the particulate fractions were first incubated in alkaline 100 mM Na_2CO_3 (pH 11.5). Under these conditions any membrane vesicles present are converted to sheets, and most protein−protein interactions are disrupted; however, protein−lipid (hydrophobic) interactions are not disrupted, and the membrane bilayer remains intact (*33*). Thus this incubation is expected to strip away most peripheral membrane proteins but to leave integrated proteins in the membrane. Following this incubation in alkaline medium the sucrose concentration of the particulate fraction was increased to 1.6 M, and the membrane fraction was prepared by flotation (see Materials and Methods). In addition to separating the membranes from the peripheral proteins removed by alkaline treatment this step also leaves any aggregated recombinant proteins arising from overexpression in the lower phase.

In Figure 3B we show the percentage of recombinant protein in the particulate fraction that was recovered in the membrane fraction for the constructs cHR 7, cHR 7−8, cHR 7−9, and cHR 7−10. As already discussed, the high level of glycosylation observed for cHR 7−10 (*15*) indicates that this protein is integrated into the membrane and, as expected, its recovery in the membrane fraction is relatively high (∼60%). On the other hand, the recovery of cHR 7 in the membrane fraction is considerably lower (<20%), consistent with previous results indicating that HR 7 does not integrate into the lipid bilayer. A similar low recovery is observed for cHR 7−8 and for EGFP-β, the (soluble) protein expressed by the empty pEGFP-β vector. These observations, together with the fact that the proteins expressed by cHR 7 and cHR 7−8 are poorly glycosylated (Figure 2A), are consistent with the hypothesis that neither HR 7 nor HR 8 is integrated into the membrane as a MSS in these two recombinant proteins. In contrast to these results, however, the recovery of the

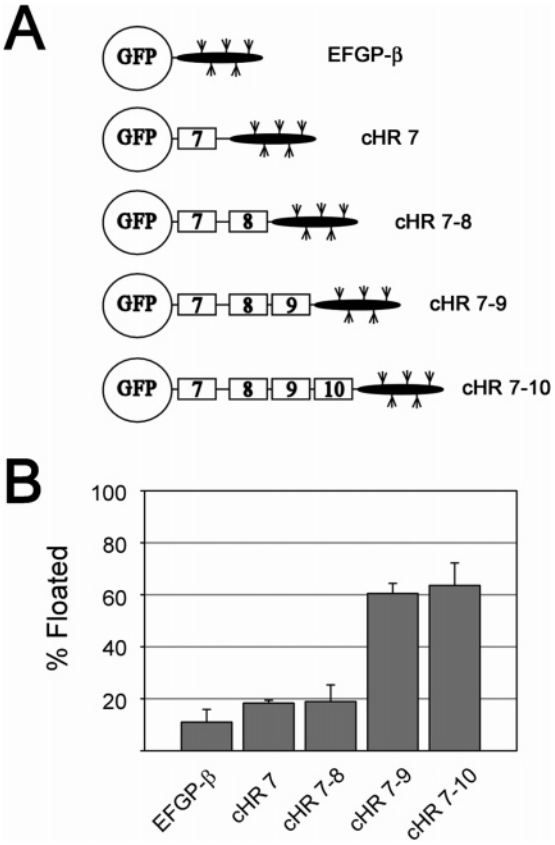

FIGURE 3: Recovery of protein in the membrane (floated) fraction. (A) Schematic representations of constructs containing no HRs (EGFP-β; the protein expressed by the empty pEGFP-β vector), HR 7 (cHR 7), HRs 7 and 8 (cHR 7−8), HRs 7−9 (cHR 7−9), and HRs 7−10 (cHR 7−10). The PS1 sequences cloned into pEGFP-β were L271−L369 (cHR 7), L271−D403 (cHR 7−8), L271−P433 (cHR 7−9), and L271−I467 (cHR 7−10). (B) For each of the constructs indicated, the percentage of recombinant protein in the particulate fraction that was recovered in the membrane fraction (% floated) is shown (determined by Western blotting and densitometry of paired particulate and membrane fractions). Note that at least some of the recovery of this latter (soluble) protein in the membrane fraction is due to contamination from the 1.6 M sucrose layer that occurs when collecting the interface between the 1.25 and 1.6 M sucrose layers (see Materials and Methods).

fusion protein expressed by cHR 7−9 in the membrane fraction is comparable to that of cHR 7−10 (Figure 3B), suggesting its efficient integration into the membrane. How this result can be reconciled with the fact that cHR 7−9 is not glycosylated is explored below.

Evidence That HR 9 Is a MSS and Induces Membrane Integration of HR 8. To further clarify the interaction of HR 9 with the membrane, we first examined the behavior of the fusion proteins encoded by cHR 7−9a and cHR 1−9a in which the PS1 sequence was terminated at G417 near the middle of HR 9 (Figure 4). These constructs extend cHR 7−8 and cHR 1−8, respectively, to include the N-terminal half of HR 9. Interestingly, although neither cHR 7−8 nor cHR 1−8 show much glycosylation (see above), both of these new recombinant proteins are highly glycosylated in HEK-293T cells (Figure 4), indicating that the N-terminal half of HR 9 by itself is capable of membrane integration with an N_{cyt}/C_{lum} orientation.

We next considered the possibility that HR 9 might participate in the formation of a hairpin-like structure that

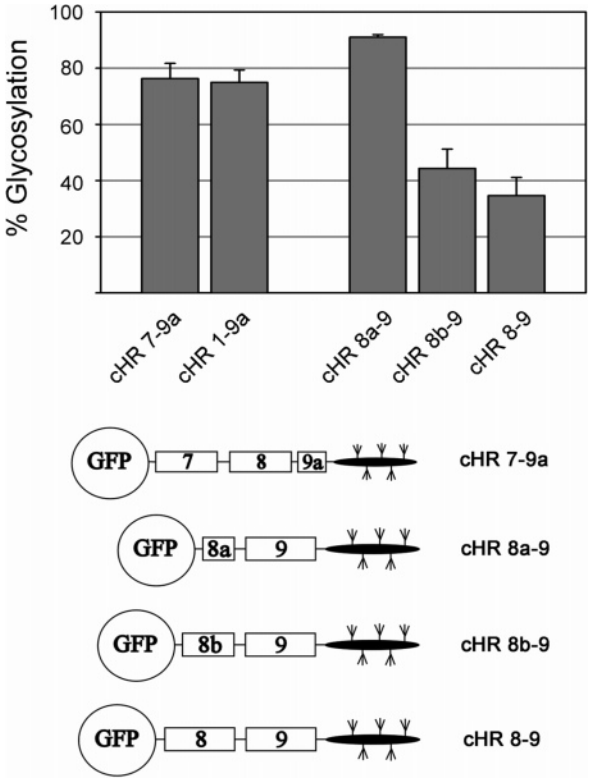

FIGURE 4: Integration of PS1 HRs 8−9. All procedures are as described in Materials and Methods and in the caption of Figure 2. The PS1 sequences cloned into pEGFP-β were L271−G417 (cHR 7−9a), M1−G417 (cHR 1−9a), L392−P433 (cHR 8a-9), D385−P433 (cHR 8b-9), and L381−P433 (cHR 8−9). Schematic illustrations of the fusion proteins are shown below the blots; cHR 1−9a (not illustrated) contains HRs 1−6 of PS1 in addition to the PS1 sequence in cHR 7−9a.

spans the membrane twice. Specifically, we wondered if HR 9 was capable of inducing forced transmembrane orientation, a phenomenon recently described by Ota et al. (*19*, *20*). These authors demonstrated that a naturally occurring MSS from the Cl^-/HCO_3^- exchanger, AE1, had such a strong tendency to assume an N_{lum}/C_{cyt} orientation that it could pull a preceding hydrophilic sequence into the membrane to form an N_{cyt}/C_{lum} MSS. To test this possibility, we added the upstream sequence from HR 8 to the construct cHR 9 which contains HR 9 and its flanking hydrophilic regions. As shown in Figure 4, as more upstream sequence from HR 8 is included in this construct (cHR 8a−9, cHR 8b−9, and cHR 8−9, respectively), its level of glycosylation systematically declines, consistent with the hypothesis that HRs 8 and 9 together assume a hairpin-like conformation.

To confirm that HR 9 does indeed independently integrate into the membrane in an N_{lum}/C_{cyt} orientation, we carried out the experiment illustrated in Figure 5A. Here we expressed HR 9 as a fusion protein preceded by a short N-terminal glycosylation tag and fused at its C-terminal end to EGFP (PS1-HR9; see Materials and Methods). The use of EGFP as a C-terminal tag in topology determinations has recently been validated by Du et al. (*34*). Their results confirm that, as expected, EGFP in a C-terminal location no longer acts as a cytosolic anchor. This is because its synthesis only begins after the synthesis and membrane integration of the preceding HRs, so the unfolded nascent EGFP peptide can pass through the translocon channel and fold in the lumen of the ER or remain in the cytosol

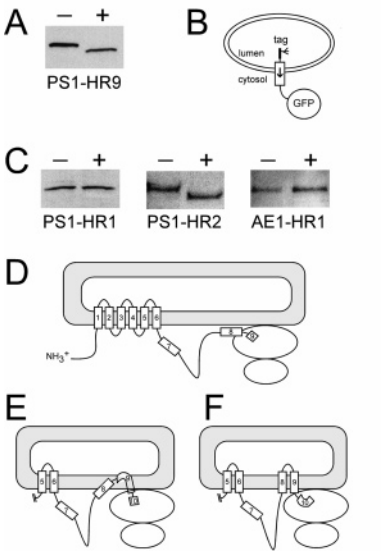

FIGURE 5: HR 9 can independently adopt an N_{lum}/C_{cyt} orientation. (A) Typical Western blot of a membrane fraction prepared from HEK-293T cells transfected with PS1-HR9 and treated with (+) or without (−) PNGase F. (B) Schematic representation of the integration of this fusion protein into the ER membrane. (C) Typical Western blots of membrane fractions prepared from HEK-293T cells transfected with PS1-HR1, PS1-HR2, and AE1-HR1 (see Materials and Methods), treated with (+) or without (−) PNGase F. Panels D−F show a schematic representation of the proposed way in which HRs 8 and 9 of PS1 enter the membrane via forced transmembrane orientation (*19*, *20*). See text for details.

according to the orientation assumed by the preceding HRs. As clearly seen in Figure 5, the construct PS1-HR9 is highly glycosylated, demonstrating that HR 9, if unconstrained by a preceding cytosolic anchor (as in Figure 2), integrates into the bilayer in an N_{lum}/C_{cyt} (type I) orientation (cf. Figure 5B). Also shown in Figure 5C are results from three control constructs, PS1-HR1, PS1-HR2, and AE1-HR1 (see Materials and Methods). In PS1-HR1 and AE1-HR1 the first hydrophobic regions of PS1 and AE1, respectively, replace HR 9 in PS1-HR9. Both of these HRs insert into the membrane in an N_{cyt}/C_{lum} orientation in their respective proteins, and consistent with this orientation neither PS1-HR1 nor AE1-HR1 is glycosylated (Figure 5C). In PS1-HR2 the second hydrophobic region of PS1 replaces HR 9 in PS1-HR9. Like PS1-HR9 this recombinant protein is highly glycosylated, consistent with a preferred N_{lum}/C_{cyt} orientation for HR 2.

In Figure 5D−F we show a schematic representation of the proposed way in which HRs 8 and 9 of PS1 enter the membrane via forced transmembrane orientation (*19*, *20*). After its synthesis, HR 8 remains on the cytosolic side of the membrane (Figure 5D). As HR 9 emerges from the ribosome, it preferentially adopts an N_{lum}/C_{cyt} orientation (Figure 5E), pulling HR 8 into the membrane as an N_{cyt}/C_{lum} MSS (Figure 5F).

MTSET Derivatization of Inserted Cysteines in PS1. To confirm that the loop between HRs 8 and 9 is indeed oriented toward the lumen of the ER, we made two full-length PS1 mutants, one in which S367 was mutated to C (S367C) and the other in which W404 was mutated to C (W404C). S367 lies in the loop between HRs 7 and 8, which is predicted to be cytosolic (see above), and W404 lies in the loop between HRs 8 and 9. Sealed cytosolic-side-out ER vesicles (*15*) were

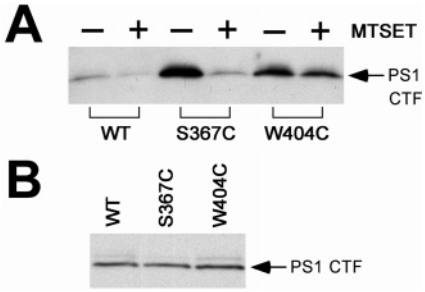

FIGURE 6: Biotinylation of cysteine mutants by biotin maleimide. (A) HEK-293 cells were stably transfected with cDNA coding for wild-type PS1 (WT) or the single cysteine PS1 mutants S367C and W404C. Cytosolic-side-out ER membrane vesicles were prepared from these cells, preincubated with (+) or without (−) membrane-impermeant sulfhydryl reagent MTSET (as indicated), and then treated with the sulfhydryl-specific membrane-permeant reagent biotin maleimide. Following solubilization, biotinylated proteins were precipitated using Neutravidin beads (see Materials and Methods for details). This material was then analyzed by Western blotting using a monoclonal antibody directed against the CTF of PS1 (Chemicon). (B) Western blot of particulate fractions (30 μg) prepared from HEK-293 cells stably expressing wild-type PS1, S367C, or W404C, illustrating similar levels of recombinant protein expression.

prepared from HEK-293 cells stably transfected with wild-type PS1, S367C, or W404C, respectively. These vesicles were first treated with or without the membrane-impermeant sulfhydryl reagent MTSET and then with the sulfhydryl-specific membrane-permeant reagent biotin maleimide; then the vesicles were solubilized, and biotinylated proteins were precipitated using Neutravidin beads (see Materials and Methods). In this protocol MTSET is expected to react mainly with exposed (cytosolic) cysteines, leaving only luminal cysteines available for biotinylation in MTSET-treated vesicles. Typical results for ER vesicles from wild-type PS1, S367C, and W404C transfected cells are shown in Figure 6; this is a Western blot of Neutravidin-precipitated material probed with an antibody against the C-terminal fragment (CTF) of PS1. In cells the PS1 holoprotein is rapidly endoproteolyzed by cleavage near Met292, resulting in a ~30 kDa N-terminal fragment and ~20 kDa CTF. The CTF contains two native cysteines, C410 and C419, both located in HR 9 (Figure 1C). Little wild-type CTF is precipitated with Neutravidin (Figure 6), indicating that neither of these native cysteines reacts strongly with biotin maleimide. This observation is consistent with the hypothesis that HR 9, and these cysteines, is buried in the membrane and thus unavailable for reaction. In contrast, the CTF from S367C reacts strongly with biotin maleimide, and this reaction is markedly blunted (89.5 ± 0.4% inhibition) by pretreatment with MTSET, consistent with the predicted cytosolic location of S367. Finally, the CTF from W404C also reacts strongly with biotin maleimide, but MTSET preincubation has relatively little effect on this reaction (21.1 ± 3.7% inhibition), consistent with a protected, presumably luminal, location for W404.

Conclusions and Relationship to Previous Topology Studies of PS1. Our conclusion that HRs 8 and 9 are MSSs in full-length PS1 is in agreement with those of Li and Greenwald (*13*, *14*), who studied the topology of SEL-12 and PS1 using expression in *C. elegans* (see introduction). Both Lehmann et al. (*11*) and Nakai et al. (*12*) argued that HRs 8 and 9 were not MSSs; however, their conclusions

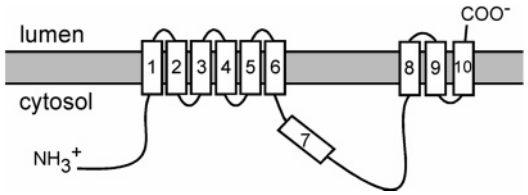

FIGURE 7: Topology model for human PS1. See text for details.

were based on interpretations of experiments involving truncation mutants similar to our constructs cHR 1−8 and cHR 1−9. These authors found that reporter peptides fused to the PS1 sequence truncated after HRs 8 and 9 were not glycosylated when expressed in the presence of dog pancreatic microsomes or in COS cells and, in addition, that these reporter peptides were susceptible to digestion by proteinase K added to the extramicrosomal (cytoplasmic) solution. In fact, we also find that our constructs truncated after HRs 8 (cHR 1−8, cHR 7−8) and 9 (cHR 1−9 and cHR 7−9) are not glycosylated (see above), and we concur that their C-termini are cytosolic. However, as discussed in detail above, our experiments strongly suggest that HRs 8 and 9 are nevertheless MSSs. Specifically, we propose that although HR 8 is unable to integrate into the membrane on its own, it is pulled into the membrane by the strong tendency of HR 9 to assume an N_{lum}/C_{cyt} orientation. Thus we differ with Lehmann et al. (*11*) and Nakai et al. (*12*) only in the interpretation of their data.

Our model for the topology of PS1 which incorporates our previously published conclusion that HR 10 is a MSS is illustrated in Figure 7.

ACKNOWLEDGMENT

We thank Dr. Bruce J. Baum for many helpful discussions during the course of this work.

REFERENCES

1. Annaert, W., and De Strooper, B. (2002) A cell biological perspective on Alzheimer's disease, *Annu. Rev. Cell Dev. Biol. 18*, 25−51.
2. Selkoe, D. J. (2001) Alzheimer's disease: genes, proteins, and therapy, *Physiol. Rev. 81*, 741−766.
3. Van Gassen, G., and Annaert, W. (2003) Amyloid, presenilins, and Alzheimer's disease, *Neuroscientist 9*, 117−126.
4. Kopan, R., and Ilagan, M. X. (2004) Gamma-secretase: proteasome of the membrane?, *Nat. Rev. Mol. Cell Biol. 5*, 499−504.
5. Fraser, P. E., Yang, D. S., Yu, G., Levesque, L., Nishimura, M., Arawaka, S., Serpell, L. C., Rogaeva, E., and George-Hyslop, P. (2000) Presenilin structure, function and role in Alzheimer disease, *Biochim. Biophys. Acta 1502*, 1−15.
6. Kim, J., and Schekman, R. (2004) The ins and outs of presenilin 1 membrane topology, *Proc. Natl. Acad. Sci. U.S.A. 101*, 905−906.
7. Doan, A., Thinakaran, G., Borchelt, D. R., Slunt, H. H., Ratovitsky, T., Podlisny, M., Selkoe, D. J., Seeger, M., Gandy, S. E., Price, D. L., and Sisodia, S. S. (1996) Protein topology of presenilin 1, *Neuron 17*, 1023−1030.
8. De Strooper, B., Beullens, M., Contreras, B., Levesque, L., Craessaerts, K., Cordell, B., Moechars, D., Bollen, M., Fraser, P., George-Hyslop, P. S., and Van Leuven, F. (1997) Phosphorylation, subcellular localization, and membrane orientation of the Alzheimer's disease-associated presenilins, *J. Biol. Chem. 272*, 3590−3598.
9. Dewji, N. N., and Singer, S. J. (1997) The seven-transmembrane spanning topography of the Alzheimer disease-related presenilin proteins in the plasma membranes of cultured cells, *Proc. Natl. Acad. Sci. U.S.A. 94*, 14025−14030.
10. Dewji, N. N., Valdez, D., and Singer, S. J. (2004) The presenilins turned inside out: implications for their structures and functions, *Proc. Natl. Acad. Sci. U.S.A. 101*, 1057−1062.
11. Lehmann, S., Chiesa, R., and Harris, D. A. (1997) Evidence for a six-transmembrane domain structure of presenilin 1, *J. Biol. Chem. 272*, 12047−12051.
12. Nakai, T., Yamasaki, A., Sakaguchi, M., Kosaka, K., Mihara, K., Amaya, Y., and Miura, S. (1999) Membrane topology of Alzheimer's disease-related presenilin 1. Evidence for the existence of a molecular species with a seven membrane-spanning and one membrane-embedded structure, *J. Biol. Chem. 274*, 23647−23658.
13. Li, X., and Greenwald, I. (1996) Membrane topology of the *C. elegans* SEL-12 presenilin, *Neuron 17*, 1015−1021.
14. Li, X., and Greenwald, I. (1998) Additional evidence for an eight-transmembrane-domain topology for *Caenorhabditis elegans* and human presenilins, *Proc. Natl. Acad. Sci. U.S.A. 95*, 7109−7114.
15. Oh, Y. S., and Turner, R. J. (2005) Evidence that the C-terminus of human presenilin 1 is located in the extra-cytoplasmic space, *Am. J. Physiol. Cell Physiol.* (in press, available on line).
16. Walter, J., Capell, A., Grunberg, J., Pesold, B., Schindzielorz, A., Prior, R., Podlisny, M. B., Fraser, P., Hyslop, P. S., Selkoe, D. J., and Haass, C. (1996) The Alzheimer's disease-associated presenilins are differentially phosphorylated proteins located predominantly within the endoplasmic reticulum, *Mol. Med. 2*, 673−691.
17. Kim, S. H., Lah, J. J., Thinakaran, G., Levey, A., and Sisodia, S. S. (2000) Subcellular localization of presenilins: association with a unique membrane pool in cultured cells, *Neurobiol. Dis. 7*, 99−117.
18. Annaert, W. G., Levesque, L., Craessaerts, K., Dierinck, I., Snellings, G., Westaway, D., George-Hyslop, P. S., Cordell, B., Fraser, P., and De, S. B. (1999) Presenilin 1 controls gamma-secretase processing of amyloid precursor protein in pre-golgi compartments of hippocampal neurons, *J. Cell Biol. 147*, 277−294.
19. Ota, K., Sakaguchi, M., von Heijne, G., Hamasaki, N., and Mihara, K. (1998) Forced transmembrane orientation of hydrophilic polypeptide segments in multispanning membrane proteins, *Mol. Cell 2*, 495−503.
20. Sakaguchi, M. (2002) Autonomous and heteronomous positioning of transmembrane segments in multispanning membrane protein, *Biochem. Biophys. Res. Commun. 296*, 1−4.
21. Dohke, Y., and Turner, R. J. (2002) Evidence that the transmembrane biogenesis of aquaporin 1 is cotranslational in intact mammalian cells, *J. Biol. Chem. 277*, 15215−15219.
22. Moore-Hoon, M. L., and Turner, R. J. (2000) The structural unit of the secretory Na^+-K^+-$2Cl^-$ cotransporter (NKCC1) is a homodimer, *Biochemistry 39*, 3718−3724.
23. Tanner, M. J., Martin, P. G., and High, S. (1988) The complete amino acid sequence of the human erythrocyte membrane anion-transport protein deduced from the cDNA sequence, *Biochem. J. 256*, 703−712.
24. Dohke, Y., Oh, Y. S., Ambudkar, I. S., and Turner, R. J. (2004) Biogenesis and topology of the transient receptor potential Ca^{2+} channel TRPC1, *J. Biol. Chem. 279*, 12242−12248.
25. Kutay, U., Ahnert-Hilger, G., Hartmann, E., Wiedenmann, B., and Rapoport, T. A. (1995) Transport route for synaptobrevin via a novel pathway of insertion into the endoplasmic reticulum membrane, *EMBO J. 14*, 217−223.
26. Feramisco, J. D., Goldstein, J. L., and Brown, M. S. (2004) Membrane topology of human insig-1, a protein regulator of lipid synthesis, *J. Biol. Chem. 279*, 8487−8496.
27. Bamberg, K., and Sachs, G. (1994) Topological analysis of H^+,K^+-ATPase using in vitro translation, *J. Biol. Chem. 269*, 16909−16919.
28. Gerelsaikhan, T., and Turner, R. J. (2000) Transmembrane topology of the secretory Na^+-K^+-$2Cl^-$ cotransporter NKCC1 studied by in vitro translation, *J. Biol. Chem. 275*, 40471−40477.
29. Bayle, D., Weeks, D., and Sachs, G. (1995) The membrane topology of the rat sarcoplasmic and endoplasmic reticulum calcium ATPases by in vitro translation scanning, *J. Biol. Chem. 270*, 25678−25684.
30. Bayle, D., Weeks, D., and Sachs, G. (1997) Identification of membrane insertion sequences of the rabbit gastric cholecystokinin-A receptor by in vitro translation, *J. Biol. Chem. 272*, 19697−19707.
31. Denzer, A. J., Nabholz, C. E., and Spiess, M. (1995) Transmembrane orientation of signal-anchor proteins is affected by the folding state but not the size of the N-terminal domain, *EMBO J. 14*, 6311−6317.

32. Goder, V., and Spiess, M. (2001) Topogenesis of membrane proteins: determinants and dynamics, *FEBS Lett. 504*, 87−93.
33. Fujiki, Y., Hubbard, A. L., Fowler, S., and Lazarow, P. B. (1982) Isolation of intracellular membranes by means of sodium carbonate treatment: application to endoplasmic reticulum, *J. Cell Biol. 93*, 97−102.
34. Du, G. G., Sandhu, B., Khanna, V. K., Guo, X. H., and MacLennan, D. H. (2002) Topology of the Ca^{2+} release channel of skeletal muscle sarcoplasmic reticulum (RyR1), *Proc. Natl. Acad. Sci. U.S.A. 99*, 16725−16730.
35. Kyte, J., and Doolittle, R. F. (1982) A simple method for displaying the hydropathic character of a protein, *J. Mol. Biol. 157*, 105−132.
36. Cserzo, M., Wallin, E., Simon, I., von Heijne, G., and Elofsson, A. (1997) Prediction of transmembrane alpha-helices in prokaryotic membrane proteins: the dense alignment surface method, *Protein Eng. 10*, 673−676.
37. Tusnady, G. E., and Simon, I. (2001) The HMMTOP transmembrane topology prediction server, *Bioinformatics 17*, 849−850.
38. Krogh, A., Larsson, B., von Heijne, G., and Sonnhammer, E. L. (2001) Predicting transmembrane protein topology with a hidden Markov model: application to complete genomes, *J. Mol. Biol. 305*, 567−580.
39. Rost, B., Fariselli, P., and Casadio, R. (1996) Topology prediction for helical transmembrane proteins at 86% accuracy, *Protein Sci. 5*, 1704−1718.
40. von Heijne, G. (1992) Membrane protein structure prediction. Hydrophobicity analysis and the positive-inside rule, *J. Mol. Biol. 225*, 487−494.
41. Hofmann, K., and Stoffel, W. (1993) TM-base—a database of membrane spanning protein segments, *Biol. Chem. Hoppe-Seyler 374*, 166−171.
42. Jones, D. T., Taylor, W. R., and Thornton, J. M. (1994) A model recognition approach to the prediction of all-helical membrane protein structure and topology, *Biochemistry 33*, 3038−3049.
43. Pasquier, C., and Hamodrakas, S. J. (1999) An hierarchical artificial neural network system for the classification of transmembrane proteins, *Protein Eng. 12*, 631−634.
44. Liu, L. P., and Deber, C. M. (1999) Combining hydrophobicity and helicity: a novel approach to membrane protein structure prediction, *Bioorg. Med. Chem. 7*, 1−7.

BI0509494